

IMPROVING THE PERFORMANCE OF SATELLITE-TO-IRRADIANCE MODELS USING THE SATELLITE'S INFRARED SENSORS

Richard Perez
ASRC, Albany, NY, 12203
Perez@asrc.cestm.albany.edu

Sergey Kivalov
ASRC, Albany, NY, 12203
skivalov@asrc.cestm.albany.edu

Jim Schlemmer
ASRC, Albany, NY, 12203
Jim@asrc.cestm.albany.edu

Charles Hemker, Jr.
ASRC, Albany, NY, 12203
kmh1@asrc.cestm.albany.edu

Antoine Zelenka
MeteoSuisse (emeritus)
Antoine.zelenka@tele2.ch

ABSTRACT

This article describes, and presents a preliminary validation of a new geostationary satellite-to-irradiance model designed to complement the existing SUNY model used in the US National Solar Resource Data Base and in SolarAnywhere. The new model uses the satellite's infrared channels to circumvent the main weakness of the current visible channel-based model: its poor performance under snow or persistent cloud conditions. Operationally the new model runs in the background when no snow cover is detected, but takes over when snow cover is detected from the existing model's data input stream.

1. INTRODUCTION

The SUNY satellite model [1, 2] has been used to produce the post-1998 part of the National Solar Resource Data Base (NSRDB, [3]) and is the main engine of new operational products such as SolarAnywhere [4]. This model performs acceptably but exhibits shortcomings under certain conditions. The most important weakness of the model is its increased uncertainty and resulting bias when the ground is covered by snow or, more generally, when the ground is highly reflective. This is because, following the fundamental relationship identified by Schmetz [5], the model uses, as its main input, the satellite's visible channel in a way that treats the darkest radiances observed at a particular location as ground seen from space (i.e., clear sky conditions) and the

brightest as clouds (i.e., overcast sky conditions). This dark-bright operational dynamics is considerably reduced when the ground is bright from snow or from local geology, and in some cases, such as fresh snow over barren land, it may even be reversed. Because the accuracy of the model depends upon a proper differentiation between cloud and ground, i.e., upon the brightness difference between the two, it deteriorates considerably under bright ground and/or snow cover conditions.

Another shortcoming recently identified by Gueymard et al. [6], and sometimes referred to as the "Eugene syndrome" occurs during prolonged periods of persistent cloud cover when the satellite does not see the ground, resulting in the model losing track of its evolving dark-bright dynamics.

This paper presents a practical approach to circumvent the shortcomings: weather geostationary satellites such as NOAA's operational GOES series also view the earth through several infrared (IR) sensors that cover complementary parts of the IR spectrum. Unlike the visible light seen by the satellite which is solar radiation reflected by the earth's surface and atmosphere, IR radiation is emitted by both and is therefore a function of the temperature of the emitting source along the line of sight. It has been shown that a combination of different IR channels could effectively discriminate between most clouds and the ground (e.g., [7, 8]) whether it is snow-covered or not. Figure 1 shows a qualitative example of a scene in North America where the visible image cannot distinguish

between the snow-covered ground and the clouds, but a simple combination of two IR channels can.

2. METHODOLOGY

The current visible model already acquires and uses ground snow cover as an auxiliary input [1]. Therefore the aim of the new model is not to detect snow but to take advantage of this information to build a stronger model. The new IR model is thus conceived as a *stand-by* model that runs in the background and takes over either when ground snow is present or when the ground is overly bright from geology. This approach lets us keep the operational strength of the current model under normal conditions. Note that other approaches under development in Europe with the MSG satellite include snow recognition as part of their algorithm (e.g., [9]) and embed the visible and IR channels in one single model.

The approach presently retained to build the IR model is purely empirical, relying on multi-site consensus least square fitting of IR-derived brightness temperatures to high-quality measurements representing distinct climatic environments in North America. All four IR channels from the GOES imager (Table 1) are used as an input to the model.

The empirical approach is retained because (1) the physical processes linking surface downwelling irradiance and IR channels are not as clear-cut as those linking it with reflected visible radiances [5]; and (2) it is an effective approach, further noting that existing operational satellite-based snow detection algorithms rely in part on empirical thresholds in their implementation (e.g., [10]).

Whereas the current visible model is self-calibrating and does not depend on evolving satellite calibrations [1], the IR model assumes that the satellite IR channels are properly calibrated and do not drift over time. This is a safe assumption because these channels, which are essentially temperature sensors, are constantly calibrated onboard from an absolute temperature source with an operational accuracy of $\pm 1\text{K}$ [11].

In addition to the four IR channels, the model also uses operational inputs already available as part of the SolarAnywhere data production stream, including zenith angle, surface temperature, and ground elevation. Surface temperature is a particularly important input which provides real time ground-truth reference to the remotely sensed brightness temperatures -- which are temperatures of the atmospheric layers seen by each IR channel, and that may or may not include the ground, depending on the channel and meteorological conditions.

The measurements used to develop the model consist of five stations from NOAA's SURFRAD network [ref] that regularly experience winter snow cover, including:

- Fort peck, Montana,
- Boulder, Colorado,
- Sioux Falls, South Dakota,
- Bondville, Illinois,
- Penn State, Pennsylvania.

These stations cover several distinct climatic environments ranging from humid (Penn State) to dry continental (Fort peck) locations, and low to high ground elevation (~2,000 m in Boulder).

The model per se consist of a polynomial least square fit of ~ 4,000 data points at the 5 sites under snow cover conditions. Figure 2 provides a snapshot of the relevance of each selected input, plotting both the T-ratio and the relative standard deviation of each coefficient extracted through the least square fitting process. The most important inputs are channel 4 and solar geometry (high T-score, very low standard deviation), followed by channel 2, elevation, channel 6 and ground temperature. IR channel 3 plays almost no role in the determination of surface irradiance – this would be expected because channel 3's spectral range covers a very strong water vapor absorption band limiting its sensing domain to the upper atmosphere.

3. PRELIMINARY VALIDATION

The IR+visible model is validated against a little over one year of data at each site spanning 1/1/09 to 1/21/10. Snow was present on the ground nearly 25% of the time in Fort Peck, and respectively 21%, 19%, 14% and 12% in Sioux Falls, Penn State, Bondville and Boulder.

Table 2 presents comprehensive model validation results for the five selected sites. Results are benchmarked against the existing all-visible model. Two sets of results are presented: (1) snow-only – in this case the new model consists exclusively of the new IR model, and, (2) all data points, when the new model is the proposed operational IR-visible combination.

The validation metrics include RMSE and MBE as well as the two statistical distribution metrics, KSI and OVER, recommended by the IEA-Task 36 [12]. KSI is the integral of the absolute difference between the modeled and measured cumulative frequency distributions. KSI is computed as % of the *Kolmogorov-Smirnoff* critical value – an allowable departure range from the cumulative distribution based upon the considered number of data

points [12]. The OVER statistics only integrates absolute differences in excess of the critical value.

Figure 3 provides visualization of Table 2's KSI and OVER statistics for the snow-cover events, while the scatter plots in Fig. 4 provide a qualitative visualization of the RMSE and MBE results also for the snow-only points when the two models differ.

4. DISCUSSION

The present investigation suggests that the new IR-based model enables a considerable operational improvement over the existing model during snow-cover conditions, reducing winter-time bias by a factor of ~ 4, while RMSEs are reduced by almost a factor of 2. The winter performance improvement translates into a considerable year-around improvement as well, with an overall RMSE reduction of nearly 20%.

Improvement is across the board for all sites in terms of RMSE and MBE. The largest improvement occurs for sites with little or no vegetation where snow cover results in bright reflecting surfaces (Sioux, Ft. Peck, and Boulder). In Penn State, where wooded land minimizes the visible snow impact in the first place, improvement is more modest. Interestingly, the new model is capable of correcting the snow bias whether it is negative (bright ground mistaken as clouds as in Fort Peck) or positive (overestimation of the dynamic range's lower bound as in Penn State).

Although the present limited validation is not fully independent – we used the same points to test and validate the model -- it is nevertheless a unique multi-site fit validated against multiple sites with differing environments, not a site-specific fit. Of course the model will have to be validated further and will probably benefit from an extension of the number of fitting sites, much like other robust semi-empirical models previously developed by the authors have shown [e.g., 13].

This empirical model is designed to work with GOES IR channels and is not directly transportable to transport to other geostationary satellites because of differences in the number and the bandwidth of their IR channels. However a similar approach would be straightforward and could be replicated with similar success.

While we have not yet tested it operationally, we believe that the model will also improve performance under other circumstances: (1) very high albedo (in this case the test would not be snow, but the visible model's dynamic range's lower bound) and (2) persistent seasonal cloud cover

Finally, since the IR-based model could also be implemented for cloud index determination when the sun is below the horizon, operational short-term forecasting will be enhanced for the first hours of the day.

5. ACKNOWLEDGEMENT

This work was done under funding from Clean Power Research.

6. REFERENCE

1. Perez R., P. Ineichen, K. Moore, M. Kmiecik, C. Chain, R. George and F. Vignola, (2002): A New Operational Satellite-to-Irradiance Model. *Solar Energy* 73, 5, pp. 307-317.
2. Perez R., P. Ineichen, M. Kmiecik, K. Moore, R. George and D. Renne, (2004): Producing satellite-derived irradiances in complex arid terrain. *Solar Energy* 77, 4, 363-370
3. Myers, D., S. Wilcox, W. Marion, R. George, M. Anderberg (2005): Broadband Model Performance for an Updated National Solar Radiation Data Base in the United States of America, Proc. Solar World Congress, International Solar Energy Society, Orlando, FL.
4. Ressler J. PV output validation with SolarAnywhere and PVSimulator, Napa, California: Clean Power Research, 2008. See also: http://www.californiasolarcenter.org/pdfs/forum/2008.2.8_SolarForum_JRessler-CPR_PVSimulatorOverview.pdf.
5. Schmetz J., (1989): Towards a Surface Radiation Climatology: Retrieval of Downward Irradiances from Satellites, *Atmospheric Research*, 23, 287-321
6. Gueymard C., and S. Wilcox, (2009): Spatial and temporal variability in the solar resource: Assessing the value of short-term measurements at potential solar power plant sites. Proc. ASES National Solar Conference, Buffalo, New York.
7. Barton H., (1988): Differentiating snow from clouds using mid-IR wavelength – an example from Ecuador. Proc. IGARS-88 Symposium, Edinburgh, Scotland (IEEE-88CH2497-6)
8. Connell, B., K. Gould and J. Purdom, (2001): High-Resolution GOES-8 Visible and Infrared Cloud Frequency Composites over Northern Florida during the Summers 1996–99. *Weather and Forecasting*, vol. 16, no6, pp. 713-724.
9. Cebeacauer T., M. Suri, and R. Perez, (2010): High performance MSG satellite model for operational solar energy applications. ASES National Solar 2010 Conference, Phoenix, Arizona

10. Duerr, B. and A. Zelenka (2009): Deriving surface global irradiance over the Alpine region from METEOSAT Second Generation data by supplementing the HELIOSAT method. *Int. Jour. of Remote Sensing* 30(22) 5821-584
11. NOAA-NESDIS, US Department of commerce (2010): <http://www.nesdis.noaa.gov/>
12. Beyer H. G., J. Polo-Martinez, M. Suri, J. L. Torres, E. Lorenz, C. Hoyer-Klick & P. Ineichen, (2008): Handbook on Benchmarking. International Energy Agency, Solar and Heating Cooling Programme, Task 36, Subtask A.
13. Perez, R., P. Ineichen, R. Seals, J. Michalsky and R. Stewart, (1990): Modeling Daylight Availability and Irradiance Components from Direct and Global Irradiance. *Solar Energy Vol. 44*, pp. 271-289

TABLE 1
GOES 12 Imager Channels

SATELLITE IMAGER CHANNEL	WAVELENGTH RANGE (μm)	GROUND RESOLUTION AT NADIR	PRIMARY DETECTION
# 1 VISIBLE	0.55 - 0.75	1 km	Clouds, albedo, smoke
# 2 SHORTWAVE IR	3.80 - 4.00	4 km	Clouds, smoke
# 3 Moisture IR	6.30 - 6.70	8 km	Clouds, water vapor
# 4 SURFACE TEMP IR	10.20 - 11.20	4 km	Clouds, water vapor, surface temperature
# 6 LONGWAVE IR*	12.80 - 13.80	4 km	Couds, water vapor

* Channel 6 replaces channel 5, centered at 12μ on previous platforms before GOES 12,

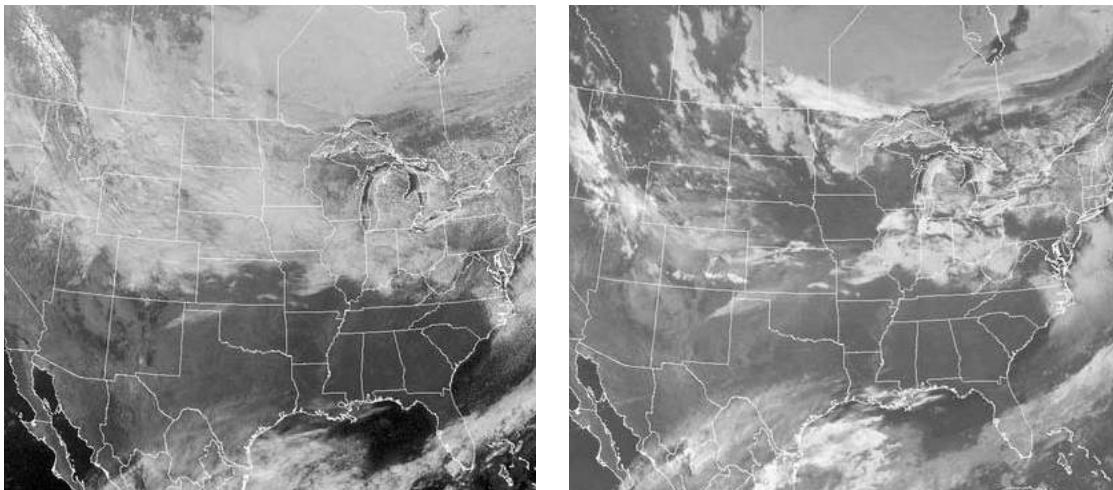


Figure 1: Comparing satellite images from the visible channel (left) and obtained by the difference of two IR channels (right). The IR view qualitatively distinguishes between snow-covered ground and clouds in the upper Great Plains.

TABLE 2
Model Performance Summary

	Fort Peck	Sioux Falls	Bondville	Boulder	Penn State
all data points					
RMSE (w/sq.m)	110	83	92	112	124
	80	66	77	100	121
MBE (w/sq.m)	-18	-2	-11	-11	17
	-1	6	-7	-3	15
KSI (%critical)	109%	57%	101%	56%	133%
	49%	48%	99%	40%	149%
OVER (%critical)	54%	11%	21%	0%	39%
	6%	9%	21%	0%	50%
snow data points					
RMSE (w/sq.m)	168	131	159	187	94
	72	71	82	114	75
MBE (w/sq.m)	-85	-51	-43	-52	21
	-18	-11	-13	9	9
KSI (%critical)	217%	106%	78%	67%	40%
	56%	62%	74%	31%	56%
OVER (%critical)	154%	61%	27%	19%	5%
	10%	11%	19%	0%	15%
Current Model		New Model			

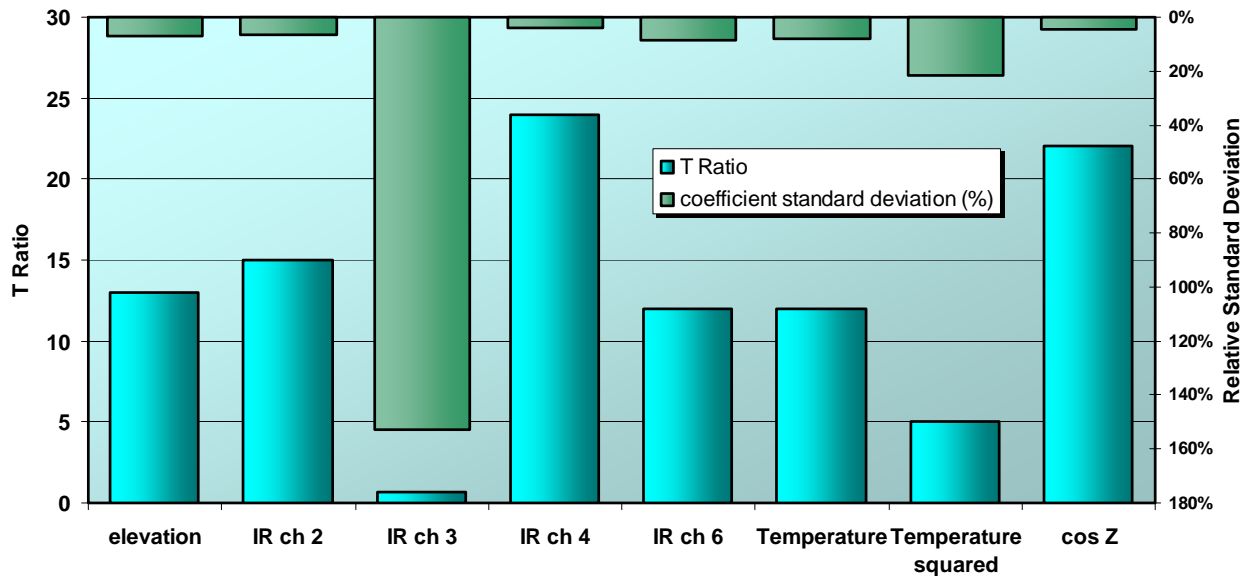


Figure 2: T-ratio and Coefficient-Standard Deviation resulting from least square fitting process

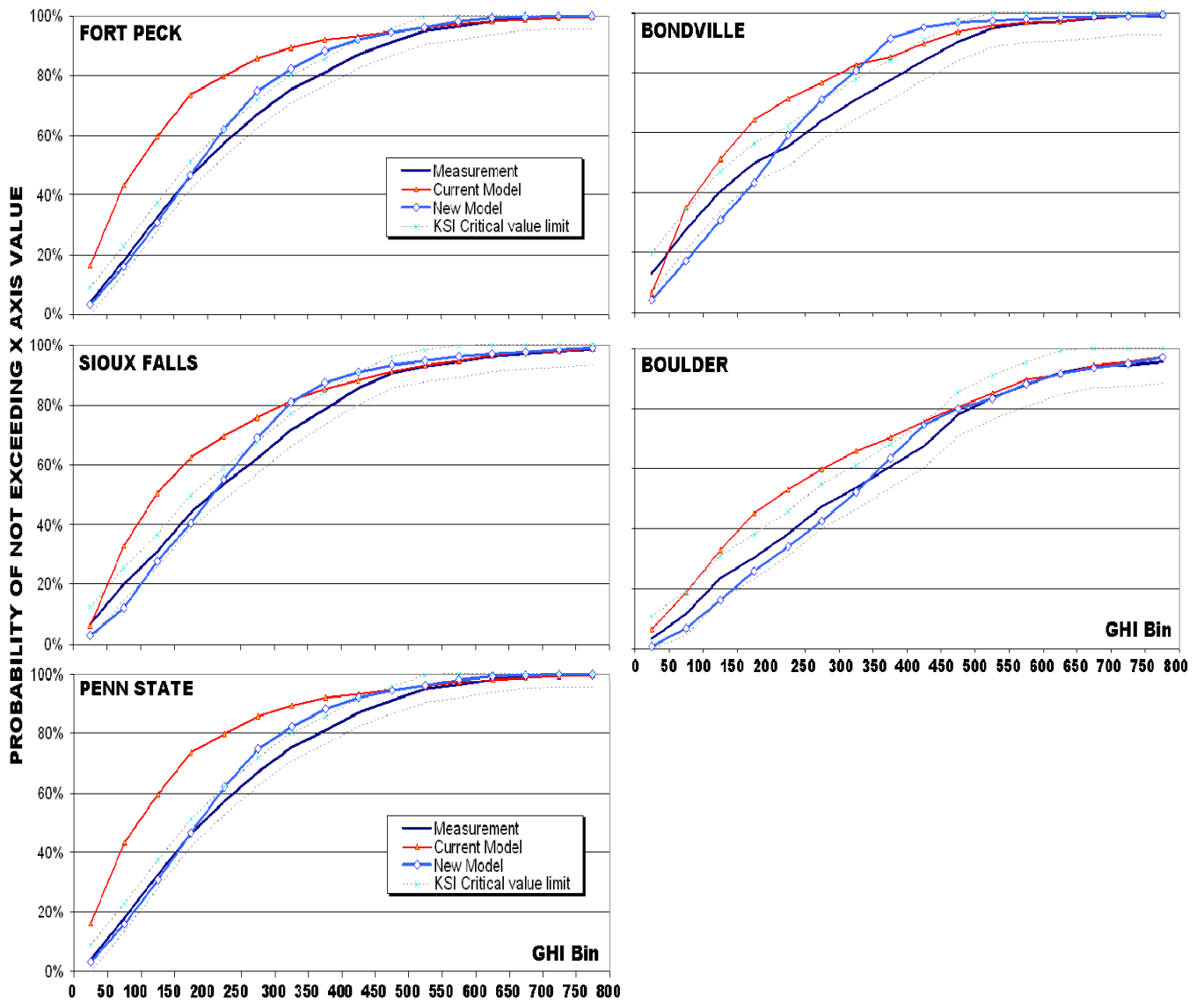


Figure 3: Cumulative Frequency distributions for measured and modeled GHI during snow cover events

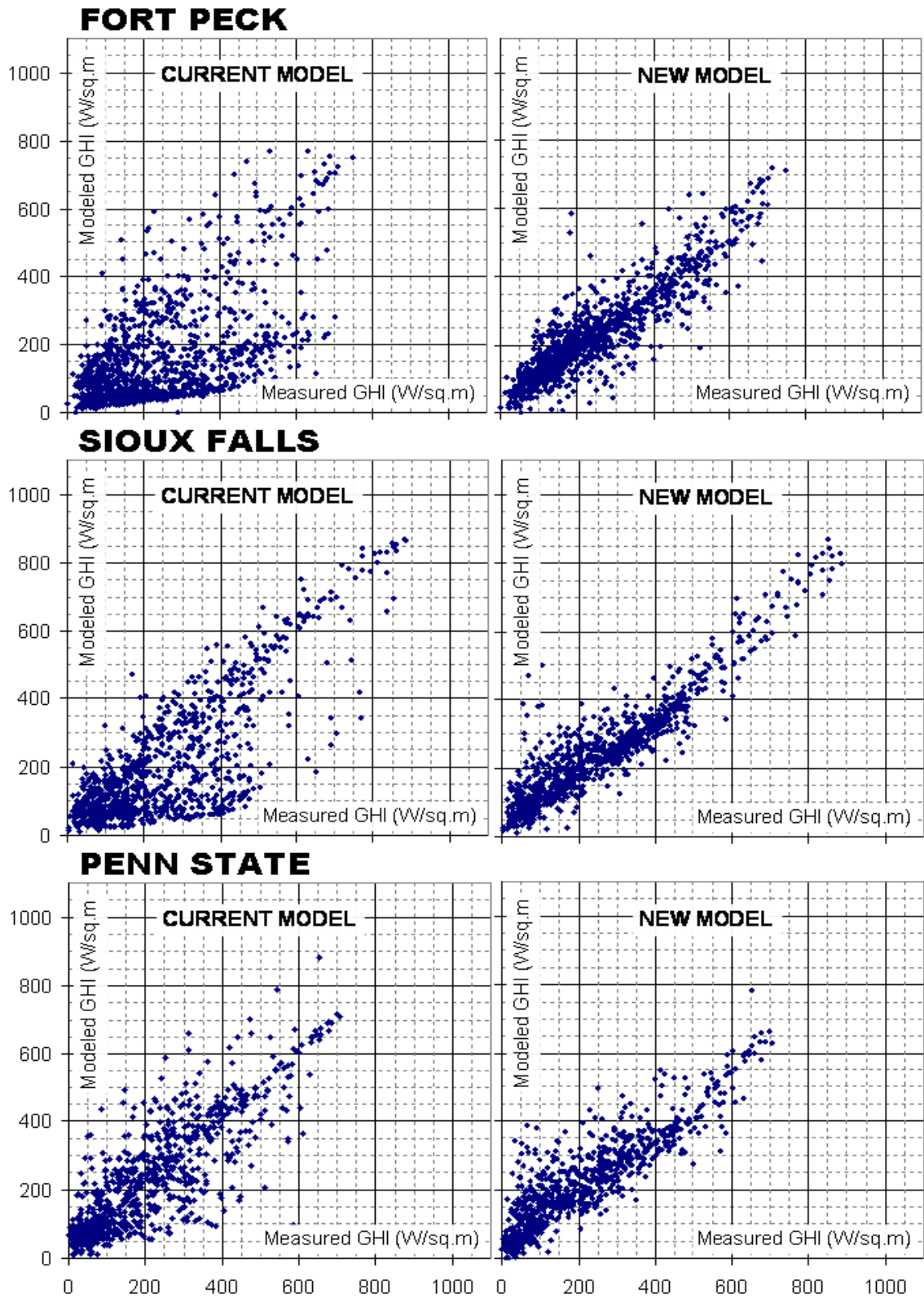


Figure 4: Modeled vs. measured GHI during snow cover events in Fort Peck, Sioux Falls and Penn State

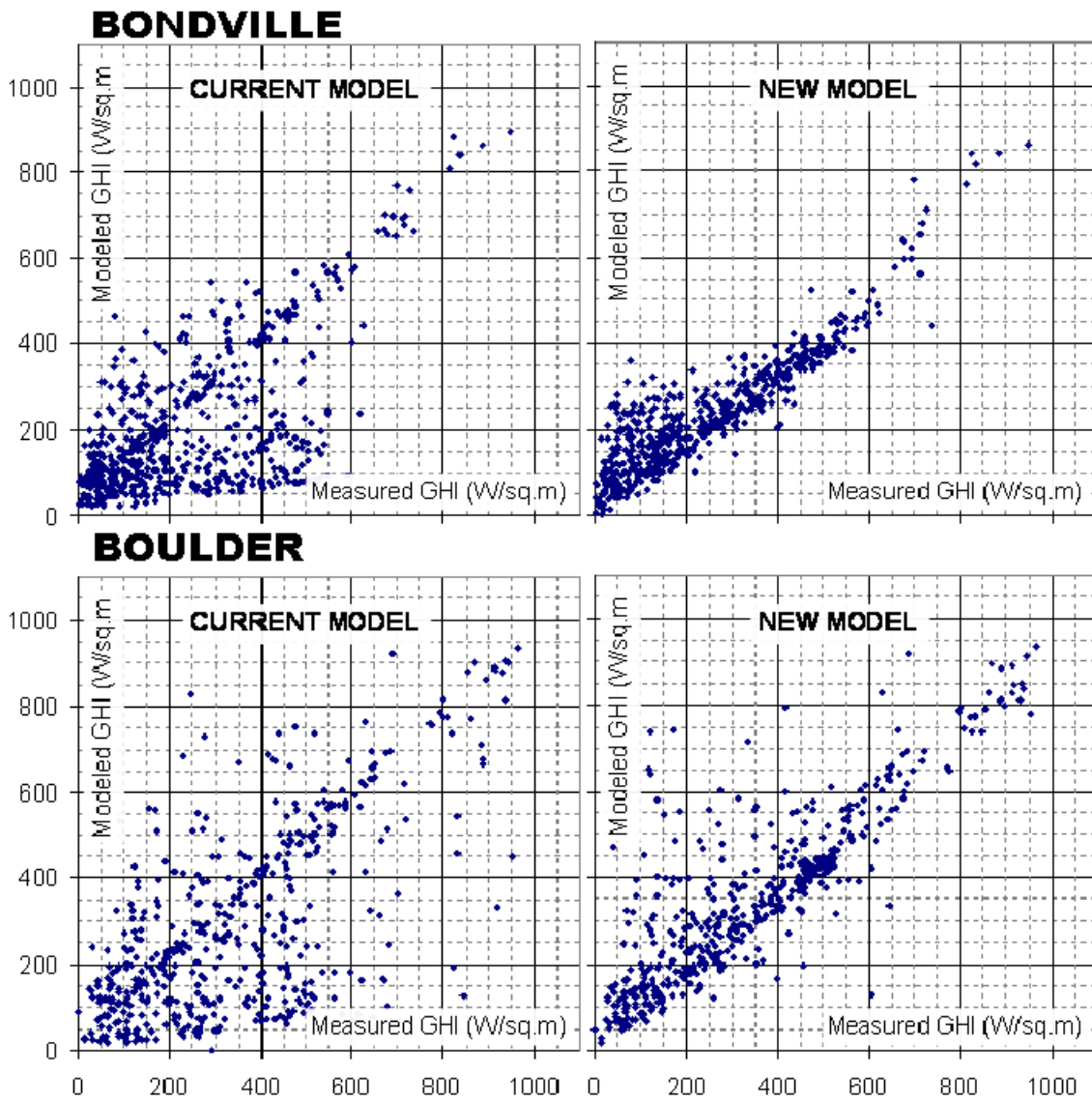


Figure 4 (continued) Bondville and Boulder